Title

Enantioselective Intramolecular Allylic Substitution via Synergistic Palladium/Chiral Phosphoric Acid Catalysis: Insight into Stereoinduction through Statistical Modeling

Journal

Angewandte Chemie International Edition, 59(34)

ISSN

1433-7851

Authors

Tsai, Cheng-Che
Sandford, Christopher
Wu, Tao
et al.

Publication Date

2020-08-17

DOI

10.1002/anie.202006237

Peer reviewed

HHS Public Access

Author manuscript

Angew Chem Int Ed Engl. Author manuscript; available in PMC 2021 August 17.

Published in final edited form as:

Angew Chem Int Ed Engl. 2020 August 17; 59(34): 14647–14655. doi:10.1002/anie.202006237.

Enantioselective Intramolecular Allylic Substitution via Synergistic Palladium/Chiral Phosphoric Acid Catalysis: Insight into Stereoinduction through Statistical Modeling**

Cheng-Che Tsai[+],
Department of Chemistry, University of California, Berkeley Berkeley, CA 94720 (USA)

Christopher Sandford[+],
Department of Chemistry, University of Utah 315 South 1400 East, Salt Lake City, UT 84112 (USA)

Tao Wu,
Department of Chemistry, University of California, Berkeley Berkeley, CA 94720 (USA)

Buyun Chen,
Department of Chemistry, University of California, Berkeley Berkeley, CA 94720 (USA)

Matthew S. Sigman[*],
Department of Chemistry, University of Utah 315 South 1400 East, Salt Lake City, UT 84112 (USA)

F. Dean Toste[*]
Department of Chemistry, University of California, Berkeley Berkeley, CA 94720 (USA)

Abstract

The mode of asymmetric induction in an enantioselective intramolecular allylic substitution reaction catalyzed by a combination of palladium and a chiral phosphoric acid was investigated by a combined experimental and statistical modeling approach. Experiments to probe nonlinear effects, the reactivity of deuterium-labeled substrates, and control experiments revealed that nucleophilic attack to the π-allylpalladium intermediate is the enantio-determining step, in which the chiral phosphate anion is involved in stereoinduction. Using multivariable linear regression analysis, we determined that multiple noncovalent interactions with the chiral environment of the phosphate anion are integral to enantiocontrol in the transition state. The synthetic protocol to form chiral pyrrolidines was further applied to the asymmetric construction of C–O bonds at fully substituted carbon centers in the synthesis of chiral 2,2-disubstituted benzomorpholines.

[**]A previous version of this manuscript has been deposited on a preprint server (https://doi.org/10.26434/chemrxiv.11965521.v1).

[*] fdtoste@berkeley.edu, sigman@chem.utah.edu.
[+]These authors contributed equally to this work.
Present address: Department of Chemistry, Tunghai University Taichung City 40704 (Taiwan)

Conflict of interest
The authors declare no conflict of interest.

Keywords

allylic substitution; asymmetric catalysis; noncovalent interactions; palladium; statistical modeling

Introduction

Chiral phosphoric acids (CPAs) serve as versatile catalysts in organocatalyzed asymmetric transformations, and as effective co-catalysts in transition metal-catalyzed reactions.[1] The combination of CPAs with transition metal catalysts imparts new reactivity (and selectivity) manifolds that are not accessible by their individual catalytic components.[2,3] Specifically, enantioselective allylic substitution reactions of nonderivatized (unactivated) allylic alcohols are desirable as a step-economic approach to the formation of key carbon–carbon and carbon–heteroatom bonds.[4] The synergy between two distinct catalysts allows for unique reactivity of these substrates, often with enhanced enantio- and diastereocontrol.[5]

As an example, CPAs were found to be effective co-catalysts for asymmetric induction in Pd-catalyzed enantioselective allylic substitutions (Scheme 1).[6] List and co-workers reported the combination of Pd and CPA catalysts in the enantioselective allylation of branched aldehydes (Scheme 1a),[6a] wherein the CPA is the sole source of chiral information responsible for enantioinduction. In contrast, CPAs have also been leveraged to enhance the enantioselectivity of an allylic substitution reaction in which the primary source of asymmetric induction is a chiral phosphoramidite ligand for Pd, as demonstrated by the groups of Gong[6c] and Beller[6d] (Scheme 1b and c, respectively). Despite the rapid development in this field, insights into the origin of asymmetric induction by CPAs in these complicated reaction processes remains challenging.[7]

In this context, we report herein our investigation into the origin of asymmetric induction in Pd/CPA-catalyzed enantioselective allylic substitutions using a combination of experimental studies and statistical modeling (Scheme 1d).[8,9] In doing so, we are able to identify noncovalent interactions (NCIs) between the substrate and chiral phosphate anion that differentiate the energy of the transition states leading to the stereoisomeric products. The knowledge gained from these mechanistic studies allows for expansion of synthetic scope to the formation of chiral benzomorpholines, a compound class containing fully substituted carbon centers.

Results and Discussion

Initial Results

We commenced our study with the Pd-catalyzed enantioselective intramolecular allylic amination of allylic alcohol **1a** with privileged CPA, (*R*)-TCYP **3**, as a co-catalyst (Table 1). For comparative purposes, we also investigated the same reaction in the absence of Pd, according to work reported by the Takasu group in which a CPA catalyzes the allylic substitution when the alcohol is replaced by an activated trichloroacetimidate leaving group, substrate **1a′**.[10]

In the initial study, the substitution of allylic alcohol **1a** was carried out in the presence of 10 mol% of both (*R*)-TCYP **3** and $Pd(PPh_3)_4$, resulting in pyrrolidine product (*S*)-**2a** in full conversion with 84% *ee* (entry 1). In contrast, the reaction of **1a′** with (*R*)-TCYP **3** under metal-free conditions gave the opposite enantiomer of the product, (*R*)-**2a**, in 78 % **ee** (entry 2). Given that the Takasu group has demonstrated that the reaction in the absence of Pd likely proceeds by nucleophilic attack on the π-system antiperiplanar to the activated leaving group (an S_N2'-type mechanism),[10a] the enantio-divergence in the presence of Pd provides evidence of a distinct mechanism. To gain insight into the origins of this enantio-divergence, control experiments were performed: the reaction of **1a** without Pd gave no product (entry 3), while the Pd/CPA-catalyzed reaction of activated substrate **1a′** gave (**S**)-**2a** in only 9% **ee** (entry 4), as a consequence of background reactivity (entry 5).

To probe the origin(s) of enantiocontrol, nonlinear effect (NLE)[11] studies of both the synergistic Pd/CPA and S_N2' reactions were performed (Figure 1). Both reactions exhibited linear correlations ($R^2 > 0.99$) between the product and catalyst *ee*, consistent with models reported by Takasu[10a] and Beller,[6d] which propose that a single CPA is involved in the enantio-determining transition state.

To enhance the enantioselectivity of the reaction, we turned our attention towards examining alternative CPA scaffolds. We recently developed a new class of CPA catalysts, doubly axially chiral phosphoric acids (DAPs), which possess a larger chiral pocket derived from two homocoupled BINOL scaffolds.[13] The use of DAPCy catalyst **4a** resulted in an increase in enantioselectivity for both the synergistic Pd/CPA and S_N2' reactions to 95% and 90% *ee*, respectively (Table 1, entries 6 and 7).

During optimization, we observed that the identity of both the DAP catalyst and the sulfonamide protecting group on the nucleophilic nitrogen of the substrate play an important role in the enantioselectivity of the reaction, with different trends associated with the two strategies. The dependency of these two modular components of the reaction presented an ideal case study for utilizing statistical modeling tools to probe the origins of enantio-divergence between the two processes.

Statistical Modeling of the Substrate Variation

In our statistical modeling approach to investigating molecular interactions in transition states,[8] parameter sets describing molecular properties of the substrate and/or catalyst are related to the enantioselectivity of the reaction, expressed as $\Delta\Delta G^{\neq}$. The combination of multiple parameters in the mathematical expression defining $\Delta\Delta G^{\neq}$ provides insight into the overlapping factors contributing to stereocontrol.

To formulate such an equation, it is first necessary to define a set of parameters that describes electronic and steric properties of the molecular structure. In this case, we opted to simulate trends in structural variation of the sulfonamide protecting group by truncating the substrate to an $ArSO_2NH_2$ group (see the Supporting Information). DFT properties of these truncated structures were collated, and, through an iterative multivariable linear regression modeling process, models describing the effect of sulfonamide variation on the

enantioselectivity were obtained. Both leave-one-out (Q^2) and external validation ($R^2_{valid.}$) statistics were used, where appropriate, to identify a statistically robust model.

A combination of the asymmetric IR stretching frequency of the NH_2 group $\nu_{NH2,asym}$ with the partial charge according to NBO on the sulfur (NBO_S) was necessary to describe the impact of the variation of the protecting group in the enantiocontrol of the S_N2' reaction (Figure 2a and b). These parameters can be compared directly with transition states computed by Takasu and co-workers,[10a] in which the asymmetric IR stretching frequency defines the propensity of the amine N–H group to undergo hydrogen-bonding to form a hydrogen bond with the phosphoric acid P=O motif in the transition state. The partial charge according to NBO on the sulfur atom predominantly describes a correctional factor for *ortho*-substituents, a steric property that results in a change in conjugation with the aromatic ring.

With agreement between our modeling and transition states computed by Takasu and co-workers in the absence of palladium, we next turned to using statistical modeling to probe the dual catalysis manifold. According to the workflow described above, we obtained a model (Figure 2c) for the protecting group variance in which the dominant parameter is the asymmetric IR stretching frequency of the SO_2 group ($\nu_{SO2,asym}$). Interestingly, this key parameter corresponds to a hydrogen bond (or other noncovalent interaction) to the protecting group oxygen in the transition state; however, this interaction is opposite in directionality to the hydrogen bond of the S_N2' mechanism identified above.

At this stage, we identified two possibilities for the origin of this discrepancy: 1) the amine is deprotonated prior to the enantio-determining step, whereby the phosphoric acid O–H binds to the SO_2 group as part of an inner-sphere Tsuji–Trost mechanism,[14] or 2) the vibrational stretching frequency is signifying a molecular interaction between the sulfonamide oxygens and an alternative hydrogen (or Lewis acid). In order to differentiate these possibilities, it was necessary to gain further insight into the mechanism of the enantio-determining step in the reaction.

To determine whether an inner- or outer-sphere Tsuji–Trost mechanism is in operation, we synthesized deuterium-labeled, enantiomerically enriched (er = 3.4/1) allylic alcohol (*S*,*E*)-**5a** along with its corresponding trichloroacetimidate derivative (*S*,*E*)-**5a′** (Figure 3a). In this experiment, an inner-sphere process should afford the *E*-isomer of the deuterated olefin, and the *Z*-isomer results from an outer-sphere process.[15] The absolute configuration of **5a** and **5a′** was determined by Mosher ester analysis, in comparison with ^{1}H NMR spectra of analogues reported in the literature (see the Supporting Information).[15c,d] In the S_N2' reaction, the cyclized product (*R*)-**6a** was obtained in 93% *ee* with 3.4:1 *Z*:*E* selectivity, consistent with a transition state in which the nucleophile attacks the **π**-system on the opposite face to the departing leaving group.

In the presence of palladium, cyclized product (*S*)-**6a** was obtained with 95% *ee* and 2.0:1 *Z*:*E* selectivity, indicative of an outer-sphere mechanism. It is notable that the minor *E*-isomer of the product is also formed in high enantioenrichment with the same absolute configuration as the *Z*-isomer. We propose that this may result from a second-order process

in Pd, in which a second Pd^0 molecule attacks the Pd^{II}–allyl intermediate, leading to a switch in the facial position of the palladium (Figure 3b).[16] Rapid π-σ-π isomerization must then occur to form the observed isomers of deuterated product. In this scenario, the reaction operates under Curtin–Hammett control, in which outer-sphere attack of the nitrogen nucleophile is enantio-determining.[17] Alternatively, the π-allylpalladium precursor to the (*S*,*E*)-isomer could be generated directly from a slightly less favorable *syn*-ionization of (*S*,*E*)-**5a**,[18] whereby formation of the Pd^{II}–allyl intermediate is enantio-determining. To examine these possibilities, we repeated the reaction with half the palladium loading, and observed an increase in selectivity to 2.6:1 *Z*:*E*, in agreement with slowing the second-order Pd process of the first scenario. From these experiments, an inner-sphere Tsuji–Trost mechanism can be excluded, and the enantio-determining attack of the nucleophile occurs through a transition state in which the DAP catalyst is a phosphate anion (having previously protonated the OH leaving group). This leads to the conclusion that the asymmetric SO_2 vibrational stretching frequency corresponds to a noncovalent interaction (NCI) other than a hydrogen bond from the phosphoric acid O–H.

With this in mind, we turned to symmetry-adapted perturbation theory (SAPT) computations to probe the energetics of an NCI to the sulfonamide oxygens.[13a,19] In this approach, the hydrogen of a benzene probe was used to determine the maximum magnitude interaction energy and corresponding equilibrium binding distance to the protecting group. The magnitude of the interaction energy was also separated into constituent energies corresponding to electrostatics, exchange interactions, induction, and dispersion. With these new parameters, an improved statistical model (Figure 3c) was afforded with the equilibrium binding distance (D_{min}), alongside a cross-term of the dispersion energy of the interaction (E_{disp}). The negative coefficient of D_{min} defines the benefit of an interaction with a smaller equilibrium distance (stronger interaction) for improved stereocontrol, while the cross-term compensates for the additional dispersion obtained with a protecting group bearing an *ortho*-substituent on the aromatic ring. Analyzing these results, the statistical modeling suggests that an NCI with the sulfonamide oxygens is the most important molecular interaction responsible for differentiating the major and minor transition states in the presence of palladium.

Statistical Modeling of the Variation in DAP Catalyst

To gain insight into the molecular interactions with the chiral phosphate anion which govern selectivity, it was necessary to consider the flexibility of the catalyst. Given the configurational flexibility of the central axis of the DAP scaffold,[13a] we subjected TAPPh*t*Bu (triply axially chiral phosphate) catalyst **4m**, where configurational flexibility is prevented, to our reaction conditions in the presence of Pd (Figure 4a), providing a direct comparison with the enantiomer of (R_a,R_a,R_a)-DAPPh*t*Bu **4e**. We observed a reduced enantioenrichment of product (*R*)-**2a** of 84%, when compared to the *ee* of (*S*)-**2a** of 93 % with **4e**.[20] While the reduced enantioselectivity may result from changes in the catalyst pocket from the additional methyl substituents, it also suggested the possibility that the higher energy (R_a,S_a,R_1)-configuration of the DAP anion may be catalytically active. We modeled both configurations separately,[21] and obtained more interpretable multivariable linear regression models with the (R_a,S_a,R_a)-configuration. With these data in agreement, it

suggests that the higher energy configuration of the catalyst may be operational. Consequently, we believe that configurational flexibility is important in successful catalysis, and we proceed to discuss molecular interactions associated with the (R_a,S_a,R_a)-configuration of the catalyst.

Parameters associated with the variation of the DAP catalysts (Figure 4a) were obtained from truncated DFT structures (see the Supporting Information). With molecular descriptors in hand, we obtained a bivariable model (Figure 4b) to describe enantiocontrol in the synergistic Pd/CPA catalytic reaction, using the combination of the partial charge according to NBO on the reactive phosphate oxygen (NBO_o) with the dihedral angle about the naphthyl–naphthyl bond ($Dihed_{Nap\text{-}Nap}$). We ascribe the dihedral angle parameter to a classification for the partial charge, where the angle alters the delocalization across the conjugated ring system. The sign of the NBO_o term leads to the conclusion that the more negative the phosphate oxygen, the lower the degree of enantiocontrol. This is consistent with the statistical modeling of the protecting groups, since it showcases the opposite trend to one expected if deprotonation of the amine represents the key defining molecular interaction. Indeed, it suggests that the major factor that controls stereochemistry is an NCI from the phosphate oxygen that stabilizes the minor transition state and leads to reduced enantioselectivity.

It is interesting to compare these predicted NCIs with transition states calculated by Jindal and Sunoj[7f] for the Pd/CPA reaction developed by List and co-workers (Scheme 1a).[6a] While statistical modeling does not enable the identification of the precise molecular interactions involved, it does highlight both an NCI from the sulfonamide oxygen that stabilizes the major transition state, and an NCI from the phosphate oxygen that stabilizes the minor transition state. In the transition states computed by Jindal and Sunoj, the greatest change in bond distances between the major and minor transition states is for an NCI between the phosphate oxygen and a hydrogen of the PPh_3 ligand, in which the bond distance is shorter (stronger NCI) in the minor transition state.[7f] While the exact nature of the system is different in this study to the work of Jindal and Sunoj, it is possible that the statistical model is describing a similar NCI.

Moving to the analysis of catalyst effects without Pd, a univariate correlation with the dihedral angle of the varied substituent was observed for DAP catalysts with a dihedral angle > 60° (Figure 4c). However, no statistically robust models were obtained to define the variance in catalysts with a dihedral angle < 60°, which is likely a consequence of the modest spread of enantioselectivity (between 2.1 and 2.4 kcal mol^{-1}). Nonetheless, we propose that the threshold effect of the dihedral angle defines the size of the catalyst pocket, whereby a larger dihedral angle leads to an increase in the pocket size and greater flexibility in substrate binding, leading to the observed reduction in enantioselectivity.

Formation of Fully Substituted Stereocenters in Benzomorpholine Motifs

Having established evidence for the proposed mechanism, we reasoned that the combination of the configurational and conformational flexibility of the DAP catalyst may allow dynamics to alleviate the constraints of a more sterically crowded transition state.[22] Consequently, we sought to apply our synergistic reaction conditions to a more demanding

bond-formation reaction, and, to test our hypothesis, we targeted the formation of 2,2-disubstituted benzomorpholines.

Chiral benzoxazines, including benzomorpholines, are important precursors in the synthesis of many bioactive natural products and pharmaceuticals.[23] In particular, 2,2-disubstituted benzoxazines are core structures in renin inhibitors developed by Pfizer.[24] However, stereocontrol in the formation of a C—O bond at a fully substituted carbon center remains challenging.[25] Although fully substituted chiral chromans have been successfullysynthesized through allylic substitution[17,26] there are no reports, to the best of our knowledge, of the formation of 2,2-disubstituted benzomorpholines via a Tsuji–Trost reaction.

To initiate this part of the study, the enantioselective intramolecular allylic substitution of allylic alcohol **7a** was carried out with 10 mol% of $Pd(PPh_3)_4$ and DAPCy **4a**, according to the previous conditions for pyrrolidine formation, affording cyclized product (*R*)-**8a** in only 25% conversion and 5% *ee* (Table 2, entry 1). Addition of water was found to improve the conversion of the reaction (entry 2),[27] and replacement of the cyclohexyl group on the DAP catalyst with an aromatic substituent (R = Ph and 4-*t*Bu-C_6H_4) led to a significant improvement in enantioselectivity (50% and 86% *ee*, entries 3 and 4). Since several DAP catalysts were ineffective in the transformation, full analysis of the catalyst variance could not be made, but models of further data presented in the Supporting Information suggest that sterics may be more significant for catalyst selection in this reaction than for pyrrolidine formation, which is in agreement with the formation of a more sterically encumbered fully substituted stereocenter. Lastly, optimization of the solvent enabled product **8a** to be isolated in 89% yield with 93% *ee* (entry 5, see the Supporting Information for details). In contrast, using privileged CPA **3** in the synergistic catalysis gave only trace product (entry 6), while the S_N2' reaction of **7a′** with DAPPh*t*Bu **4e** gave the opposite enantiomer, (*S*)-**8a**, in 24% conversion and only 15% *ee* (entry 7). These comparative results demonstrate the power of the DAP family of catalysts to expand the synthetic applications of CPA catalysis beyond those of existing scaffolds.

We next investigated the scope of the reaction (Figure 5a), and determined that the protecting group on the amine was again important for enantiocontrol (**8b–e**), even though variation is distal to the bond-forming centers. Additionally, manipulations of the phenol substituents were found to be significant for enantioselectivity (**8a**,**b**, **8f**,**p**); the introduction of *para* electron-withdrawing groups led to significant erosion of enantioselectivity (3% *ee* for **8n**). Correlating the result of variance in both the phenol substitution and protecting group, we found a strong correlation between $\Delta\Delta G^{\neq}$ and the HOMO energy, indicative of the requirement for a highly nucleophilic phenoxide for enantiocontrol (Figure 5b). This suggests that the protecting group can be used to modulate the enantioselectivity of the reaction through orbital control, rather than through the adoption of noncovalent interactions, as observed in the above study of pyrrolidine formation. Despite the different demands on the transition states imposed by the two substrate classes studied, the flexibility of the DAP catalyst family enables the phosphate anion to afford reactivity and selectivity in both settings.

Finally, to test the limitation of the substrate scope, the methyl group in allylic alcohol **7a** was replaced by alternative substituents. Changing to either a hydrogen atom or ethyl substituent did not inhibit cyclization, affording products **8r** and **8t** in 86% yield with 83% *ee*, and 68% yield with 84% *ee*, respectively. However, allylic alcohols **7u** and **7v**, with benzyl or phenyl substituents, were unreactive under the standard reaction conditions, representing the limits of our current approach.

Conclusion

We report herein mechanistic studies on the asymmetric induction of Pd/CPA-catalyzed enantioselective allylic substitutions. Several notable observations and conclusions can be drawn from these studies: 1) CPAs catalyze both palladium- and Brønsted acid catalyzed allylic substitution reactions with high enantioselectivity. 2) Deuterium-labeling experiments are consistent with an outer-sphere nucleophilic addition to a **π**-allylpalladium intermediate, in which the CPA acts as a chiral anion in the enantio-determining step. In contrast, the CPA directly participates in the Brønsted acid catalyzed S_N2'-type substitution. Overall, these divergent mechanistic paradigms allow for the preparation of both enantiomers of the product using a single enantiomer of the CPA catalyst. 3) The origin of this enantio-divergence was investigated by statistical modeling, providing correlations to understand the noncovalent interactions for both reaction pathways. Remarkably, catalyst flexibility allows the CPA to adapt to leverage these NCIs, despite the different requirements for enantioselectivity in each. 4) Finally, the Pd/CPA-catalyzed reaction allowed for the asymmetric construction of C—O bonds at fully substituted carbon centers, giving challenging chiral 2,2-disubstituted benzomorpholine motifs. In combination, these results highlight that chiral phosphoric acid catalysis with DAPs, in both palladium and direct phosphate catalysis, enables unique reactivity in accessing both divergent enantioselectivity with a single catalyst and unprecedented access to tertiary ether stereocenters.

Supplementary Material

Refer to Web version on PubMed Central for supplementary material.

Acknowledgements

F.D.T. thanks the National Institutes of Health (R35 GM118190) and M.S.S. thanks the National Institutes of Health (GM121383) for support of this work. C.-C.T. thanks the Ministry of Science and Technology, Taiwan, for a postdoctoral fellowship (106-2917-I-564-056). C.S. thanks the EU for Horizon 2020 Marie Skłodowska-Curie Fellowship (grant no. 789399). Resources from the Center for High Performance Computing at the University of Utah, and the Extreme Science and Engineering Discovery Environment (XSEDE, supported by the NSF (ACI-1548562) and provided through allocation TG-CHE190060), are gratefully acknowledged. We thank Dr. Javier Arenas and Dr. Suhong Kim (Berkeley), Dr. Tobias Gensch (Utah), Ms. Soumi Trebedi and Prof. Raghaven Sunoj (IIT Bombay), for useful discussions.

References

[1]. a)For reviews on CPAs in asymmetric catalysis, see: Parmar D, Sugiono E, Raja S, Rueping M, Chem. Rev 2014, 114, 9047; [PubMed: 25203602] b)Zamfir A, Schenker S, Freund M, Tsogoeva SB, Org. Biomol. Chem 2010, 8, 5262. [PubMed: 20820680]

[2]. For a review on transition metal/CPA combined catalysis, see: Fang G-C, Cheng Y-F, Yu Z-L, Li Z-L, Liu X-Y, Top. Curr. Chem 2019, 377, 23.

[3]. a)For examples of transition metal/CPA combined catalysis, see: Reddi Y, Tsai C-C, Avila CM, Toste FD, Sunoj RB, J. Am. Chem. Soc 2019, 141, 998; [PubMed: 30562010] b)Avila CM, Patel JS, Reddi Y, Saito M, Nelson HM, Shunatona HP, Sigman MS, Sunoj RB, Toste FD, Angew. Chem. Int. Ed 2017, 56, 5806;Angew. Chem 2017, 129, 5900;c)Terada M, Ota Y, Li F, Toda Y, Kondoh A, J. Am. Chem. Soc 2016, 138, 11038; [PubMed: 27490239] d)Lin J-S, Dong X-Y, Li T-T, Jiang N-C, Tan B, Liu X-Y, J. Am. Chem. Soc 2016, 138, 9357; [PubMed: 27414501] e)Narute S, Parnes R, Toste FD, Pappo D, J. Am. Chem. Soc 2016, 138, 16553; [PubMed: 27959518] f)Nelson HM, Williams BD, Miro J, Toste FD, J. Am. Chem. Soc 2015, 137, 3213; [PubMed: 25723255] g)Saito K, Kajiwara Y, Akiyama T, Angew. Chem. Int. Ed 2013, 52,13284;Angew. Chem 2013, 125, 13526;h)Zhou S, Fleischer S, Junge K, Beller M, Angew. Chem. Int. Ed 2011, 50, 5120;Angew. Chem 2011, 123, 5226;i)Zhao B, Du H, Shi Y, J. Org. Chem 2009, 74, 8392; [PubMed: 19827794] j)Hamilton GL, Kang EJ, Mba M, Toste FD, Science 2007, 317, 496. [PubMed: 17656720]

[4]. a)For reviews on transition-metal-catalyzed substitutions of allylic alcohols, see: Rössler SL, Petrone DA, Carreira EM, Acc. Chem. Res 2019, 52, 2657; [PubMed: 31243973] b)Butt NA, Zhang W, Chem. Soc. Rev 2015, 44, 7929; [PubMed: 26293479] c)Sundararaju B, Achard M, Bruneau C, Chem. Soc. Rev 2012, 41, 4467. [PubMed: 22576362]

[5]. a)For examples of dual catalyzed substitutions of allylic alcohols, see: Su Y-L, Han Z-Y, Li Y-H, Gong L-Z, ACS Catal. 2017, 7,7917;b)Yoshida M, J. Org. Chem 2017, 82, 12821; [PubMed: 29047274] c)Zhou H, Zhang L, Xu C, Luo S, Angew. Chem. Int. Ed 2015, 54, 12645;Angew. Chem 2015, 127, 12836;d)Næsborg L, Halskov KS, Tur F, Mønsted SMN, Jørgensen KA, Angew. Chem. Int. Ed 2015, 54, 10193;Angew. Chem 2015, 127, 10331;e)Krautwald S, Sarlah D, Schafroth MA, Carreira EM, Science 2013, 340, 1065. [PubMed: 23723229]

[6]. a)For examples of dual catalyzed enantioselective allylic substitutions with Brønsted acids, see: Jiang G, List B, Angew. Chem. Int. Ed 2011, 50, 9471;Angew. Chem 2011, 123, 9643;b)Mukherjee S, List B, J. Am. Chem. Soc 2007, 129, 11336; [PubMed: 17715928] c)Tao Z-L, Zhang W-Q, Chen D-F, Adele A, Gong L-Z, J. Am. Chem. Soc 2013, 135, 9255; [PubMed: 23734612] d)Banerjee D, Junge K, Beller M, Angew. Chem. Int. Ed 2014, 53, 13049;Angew. Chem 2014, 126, 13265.

[7]. a)Tribedi S, Hadad CM, Sunoj RB, Chem. Sci 2018, 9, 6126; [PubMed: 30090300] b)Liu H, Duan J-X, Qu D, Guo L-P, Xie Z-Z, Organometallics 2016, 35, 2003;c)Hopmann KH, Chem. Eur. J 2015, 21, 10020; [PubMed: 26039958] d)Jindal G, Sunoj RB, Org. Lett 2015, 17, 2874; [PubMed: 26057464] e)Jindal G, Sunoj RB, J. Am. Chem. Soc 2014, 136, 15998; [PubMed: 25348704] f)Jindal G, Sunoj RB, J. Org. Chem 2014, 79, 7600. [PubMed: 25050786]

[8]. a)For reviews, see: Santiago CB, Guo J-Y, Sigman MS, Chem. Sci 2018, 9, 2398; [PubMed: 29719711] b)Toste FD, Sigman MS, Miller SJ, Acc. Chem. Res 2017, 50, 609. [PubMed: 28945415]

[9]. a)For examples, see: Kwon Y, Li J, Reid JP, Crawford JM, Jacob R, Sigman MS, Toste FD, Miller SJ, J. Am. Chem. Soc 2019, 141, 6698; [PubMed: 30920223] b)Orlandi M, Coelho JAS, Hilton MJ, Toste FD, Sigman MS, J. Am. Chem. Soc 2017, 139, 6803; [PubMed: 28475315] c)Milo A, Neel AJ, Toste FD, Sigman MS, Science 2015, 347, 737. [PubMed: 25678656]

[10]. a)Kuroda Y, Harada S, Oonishi A, Yamaoka Y, Yamada K, Takasu K, Angew. Chem. Int. Ed 2015, 54, 8263;Angew. Chem 2015, 127, 8381;for other examples of Brønsted acid catalyzed enantioselective S_N2' reactions, see: b) Kayal S, Kikuchi J, Shimizu M, Terada M, ACS Catal. 2019, 9, 6846;$_N$c)Shimizu M, Kikuchi J, Kondoh A, Terada M, Chem. Sci 2018, 9, 5747. [PubMed: 30079184]

[11]. Satyanarayana T, Abraham S, Kagan HB, Angew. Chem. Int. Ed 2009, 48, 456;Angew. Chem 2009, 121, 464.

[12]. Catalyst **3** was formulated in 0–80% ee from mixtures of (*R*)- and (*S*)-TCYP, resulting in a small error in absolute enantiopurity which explains the non-zero product *ee* in reactions with 0% *ee* catalyst.

[13]. a)Miró J, Gensch T, Ellwart M, Han S-J, Lin H-H, Sigman MS, Toste FD, J. Am. Chem. Soc 2020, 142, 6390; [PubMed: 32182422] b)Hiramatsu K, Honjo T, Rauniyar V, Toste FD, ACS Catal. 2016, 6,151;c)Honjo T, Phipps RJ, Rauniyar V, Toste FD, Angew. Chem. Int. Ed 2012, 51, 9684;Angew. Chem 2012, 124, 9822;d)Guo Q-S, Du D-M, Xu J, Angew. Chem. Int. Ed 2008, 47, 759;Angew. Chem 2008, 120, 771.

[14]. a)Hu L, Cai A, Wu Z, Kleij AW, Huang GA, Angew. Chem. Int. Ed 2019, 58, 14694;Angew. Chem 2019, 131, 14836;b)Keith JA, Behenna DC, Sherden N, Mohr JT, Ma S, Marinescu SC, Nielsen RJ, Oxgaard J, Stoltz BM, Goddard WA, J. Am. Chem. Soc 2012, 134, 19050. [PubMed: 23102088]

[15]. a)Bai D-C, Yu F-L, Wang W-Y, Chen D, Li H, Liu Q-R, Ding C-H, Chen B, Hou X-L, Nat. Commun 2016, 7, 11806; [PubMed: 27283477] b)Chen J-P, Peng Q, Lei B-L, Hou X-L, Wu Y-D, J. Am. Chem. Soc 2011, 133, 14180; [PubMed: 21827171] c)Cannon JS, Olson AC, Overman LE, Solomon NC, J. Org. Chem 2012, 77, 1961; [PubMed: 22316285] d)Cannon JS, Kirsch SF, Overman LE, Sneddon HF, J. Am. Chem. Soc 2010, 132, 15192. [PubMed: 20942424]

[16]. a)Akkarasamiyo S, Sawadjoon S, Orthaber A, Samec JSM, Chem. Eur. J 2018, 24, 3488; [PubMed: 29178406] b)Trost BM, Toste FD, J. Am. Chem. Soc 2003, 125, 3090; [PubMed: 12617676] c)Granberg KL, Bäckvall J-E, J. Am. Chem. Soc 1992, 114, 6858.

[17]. Trost BM, Shen HC, Dong L, Surivet J-P, Sylvain C, J. Am. Chem. Soc 2004, 126, 11966. [PubMed: 15382932]

[18]. a)Wolf LM, Thiel W, J. Org. Chem 2014, 79, 12136; [PubMed: 25268877] b)Kurosawa H, Kajimaru H, Ogoshi S, Yoneda H, Miki K, Kasai N, Murai S, Ikeda I, J. Am. Chem. Soc 1992, 114, 8417.

[19]. a)Emamian S, Lu T, Kruse H, Emamian H, J. Comput. Chem 2019, 40, 2868; [PubMed: 31518004] b)Parker TM, Burns LA, Parrish RM, Ryno AG, Sherrill CD, J. Chem. Phys 2014, 140, 094106; [PubMed: 24606352] c)Hohenstein EG, Sherrill CD, WIREs Comput. Mol Sci 2012, 2, 304.

[20]. TAPPhtBu 4m was used in the formation of products 8a and 8s (Figure 5), resulting in –71% *ee* (29% conversion) and –50% *ee* (50% conversion), respectively. As with the pyrrolidine cyclization, the ee was reduced in magnitude when compared to the same reaction with DAPPh*t*Bu **4e**.

[21]. For models utilizing parameters obtained from the (R_a,R_a,R_a)-configurations, see Supporting Information.

[22]. Crawford JM, Sigman MS, Synthesis 2019, 51, 1021. [PubMed: 31235980]

[23]. a)Shen H-C, Wu Y-F, Zhang Y, Fan L-F, Han Z-Y, Gong L-Z, Angew. Chem. Int. Ed 2018, 57, 2372;Angew. Chem 2018, 130, 2396;b)Pawliczek M, Shimazaki Y, Kimura H, Oberg KM, Zakpur S, Hashimoto T, Maruoka K, Chem. Commun 2018, 54, 7078;c)Hu N, Li K, Wang Z, Tang W, Angew. Chem. Int. Ed 2016, 55, 5044;Angew. Chem 2016, 128, 5128.

[24]. Powell NA, Ciske FL, Cai C, Holsworth DD, Mennen K, Van Huis CA, Jalaie M, Day J, Mastronardi M, McConnell P, Mochalkin I, Zhang E, Ryan MJ, Bryant J, Collard W, Ferreira S, Gu C, Collins R, Edmunds JJ, Bioorg. Med. Chem 2007, 15, 5912. [PubMed: 17574423]

[25]. Khan A, Khan S, Khan I, Zhao C, Mao Y, Chen Y, Zhang YJ, J. Am. Chem. Soc 2017, 139, 10733. [PubMed: 28727424]

[26]. a)Uria U, Vila C, Lin M-Y, Rueping M, Chem. Eur. J 2014, 20, 13913; [PubMed: 25201099] b)Trost BM, Shen HC, Dong L, Surivet J-P, J. Am. Chem. Soc 2003, 125, 9276. [PubMed: 12889940]

[27]. Kinoshita H, Shinokubo H, Oshima K, Org. Lett. 2004, 6, 4085. [PubMed: 15496105]

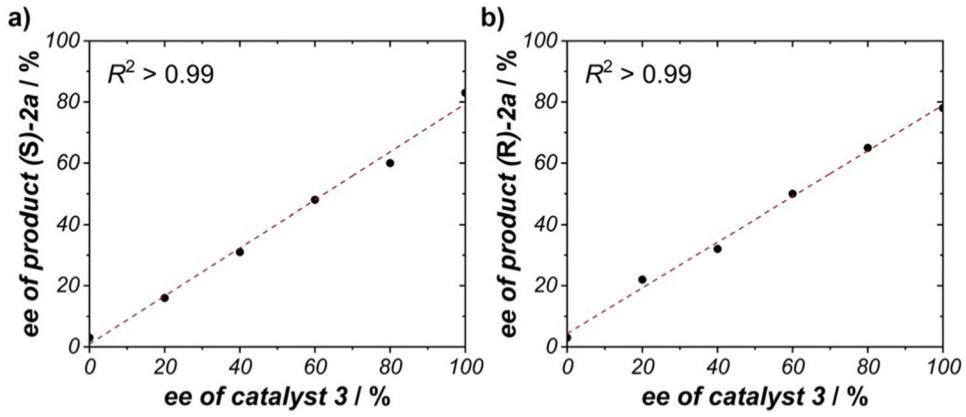

Figure 1.

Nonlinear effect studies comparing the *ee* of (*R*)-TCYP **3** with the *ee* of the product (*R*/*S*)-**2a**, both a) in the presence of $Pd(PPh_3)_4$ with substrate **1a**, and b) in the absence of $Pd(PPh_3)_4$ with substrate **1a′**. Conditions are the same as in Table 1, entries 1 and 2, respectively.[12]

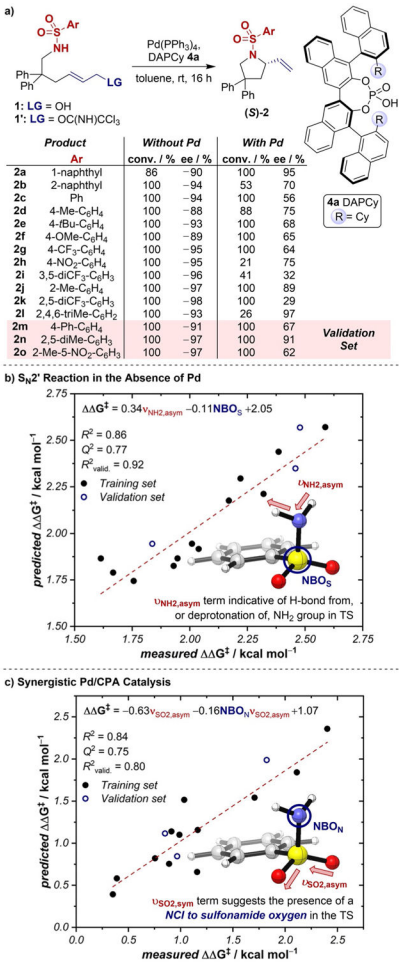

Figure 2.

a) Variance of the nitrogen protecting group. b) Model describing the protecting group variance in the absence of Pd, in which (*R*)-**2** is formed as the major enantiomer. c) Model describing the protecting group variance in the presence of Pd, in which (*S*)-**2** is formed as the major enantiomer.

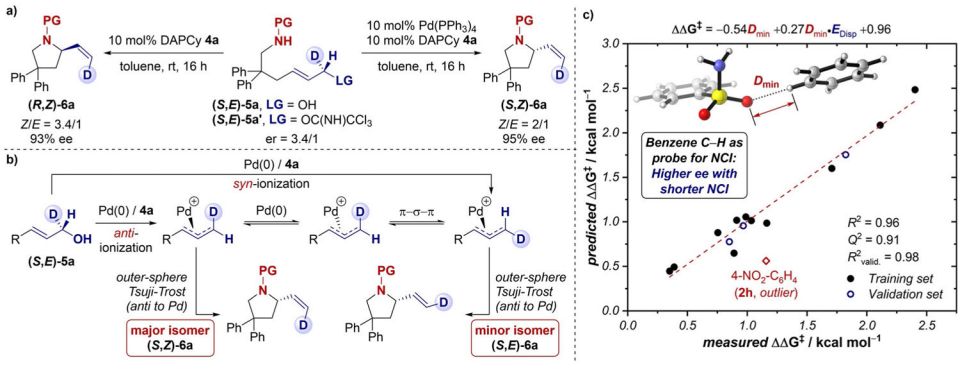

Figure 3.

a) Deuterium-labeling experiment to probe outer- or inner-sphere Tsuji–Trost mechanism. PG = SO_2-1-naphthyl. b) Rationale for major and minor isomers in the presence of palladium. c) Model for protecting group variance in the presence of palladium using parameters derived from SAPT computations. Outlier **2h** was generated from **1h**, which was not fully soluble in the reaction mixture, and is not included in the correlation statistics (also an outlier in Figure 2c).

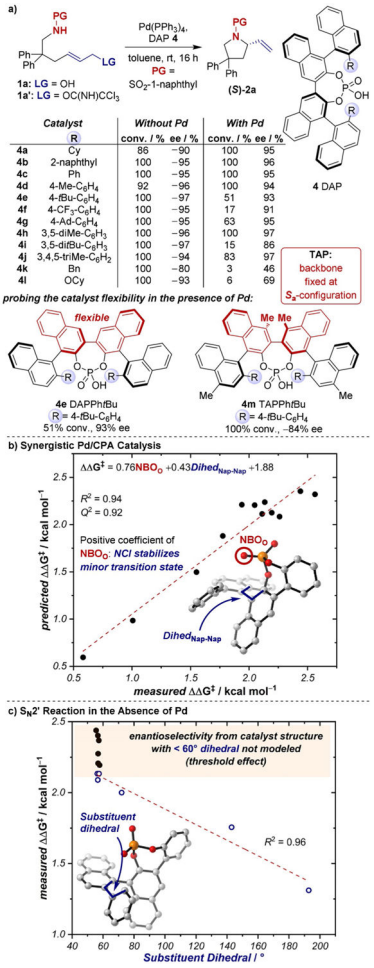

Figure 4.

a) Variance of DAP and TAP catalysts. b) Model describing the DAP catalyst variance In the presence of Pd, in which (*S*)-**2a** is formed as the major enantiomer. c) Model describing the DAP catalyst variance in the absence of Pd, in which (*R*)-**2a** is formed as the major enantiomer.

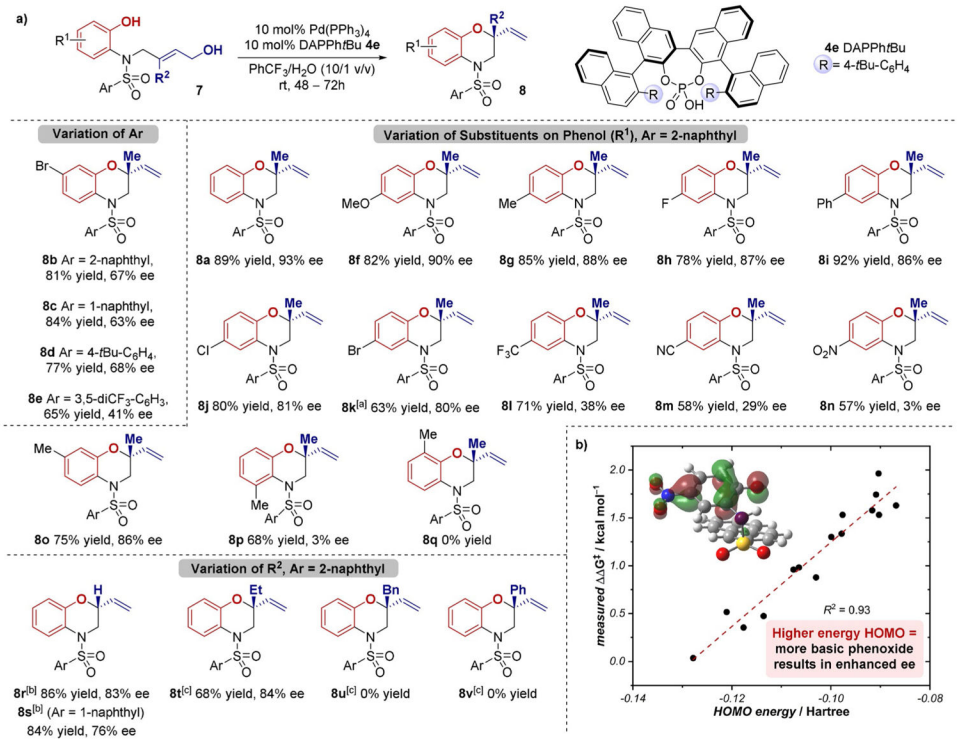

Figure 5.

a) Scope of benzomorpholine synthesis. The reaction was carried out with 10 mol% of $Pd(PPh_3)_4$ and DAPPh*t*Bu **4e** in $PhCF_3/H_2O$ (10/1 v/v) at ambient temperature. Duration of reaction was 48 h, except for **8e**, **8m**, **8n**, **8p**, and **8t**, for which the duration was 72 h. Yields reported are yields of isolated products, *ee* was determined using HPLC equipped with a chiral column.[a] $PhCF_3$ was used as solvent. [b] Toluene was used as solvent. [c] Toluene/H_2O (10/1 v/v) was used as solvent. b) Correlation of enantioselectivity with the HOMO energy for substrates **8a**–**o**. **8p** was excluded as the only example with significantly altered steric properties.

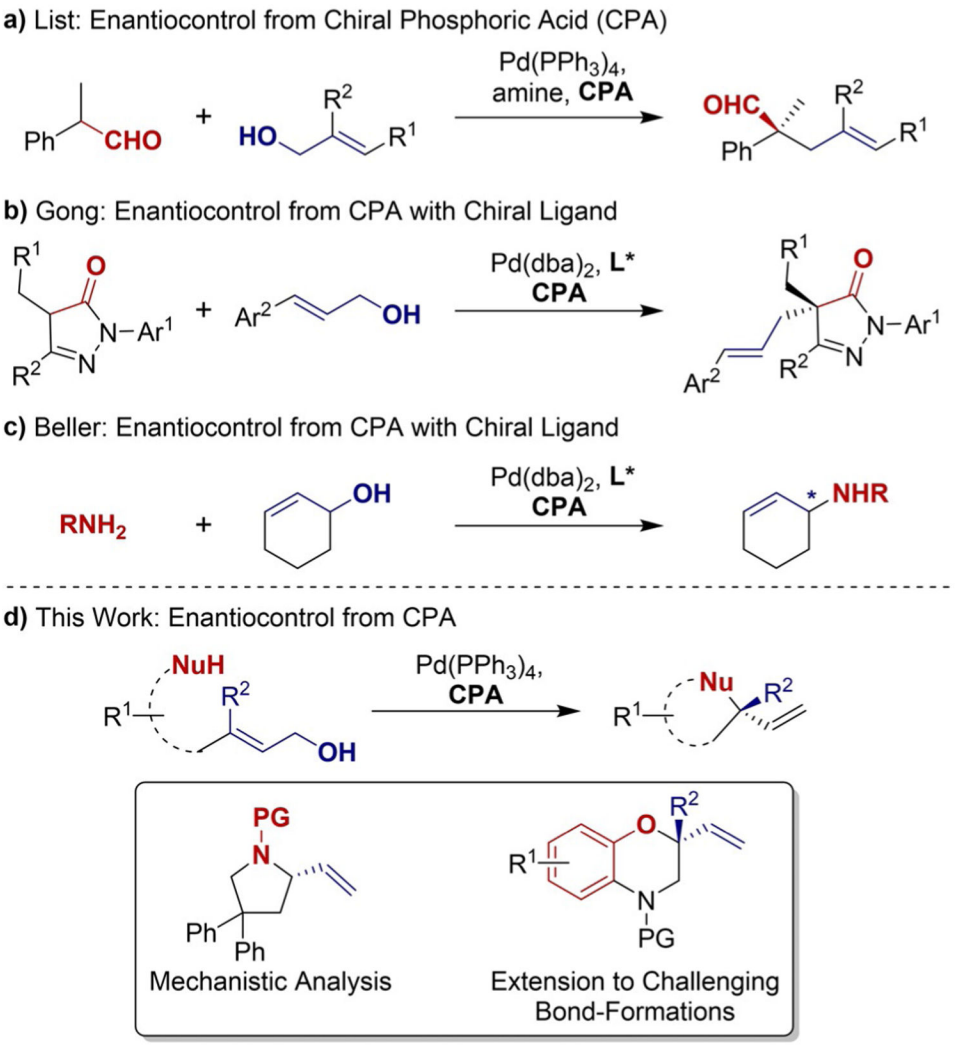

Scheme 1.

a–c) Literature examples of synergistic Pd/CPA-catalyzed enantioselective allylic substitutions of unactivated alcohols. d) Intramolecular reactions studied herein.

Table 1:

Initial results and control experiments for intramolecular substitutions.[a]

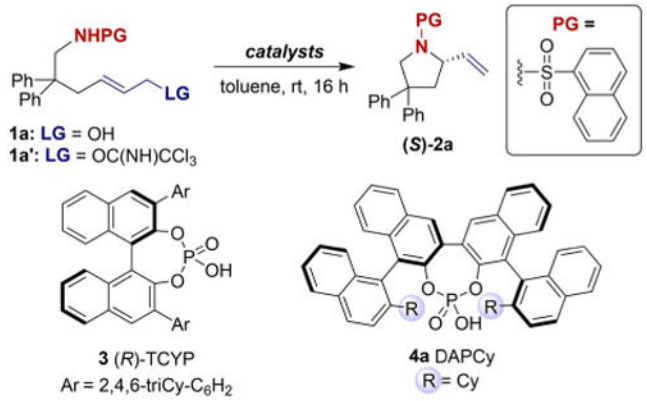

Entry	Substrate	Catalyst(s)	Conv. [%][b]	*ee* [%][c]
1	**1a**	$Pd(PPh_3)_4$/**3**	100	84
2	**1a**′	**3**	100	−78
3	**1a**	**3**	0	n.d.
4	**1a**′	$Pd(PPh_3)_4$/**3**	100	9
5	**1a**′	$Pd(PPh_3)_4$	70	0
6	**1a**	$Pd(PPh_3)_4$/**4a**	100 (85)	95
7	**1a**′	**4a**	86 (77)	−90

[a]The reaction was carried out with 10 mol% of $Pd(PPh_3)_4$ and/or CPA **3**/**4a** in toluene at ambient temperature.

[b]Conv. represents conversion measured by crude ^1H NMR analysis; yields of isolated product in parentheses.

[c]*ee* of product **2a**, determined using HPLC equipped with a chiral column, wherein a positive *ee* corresponds to (*S*)-**2a**, and a negative *ee* to (*R*)-**2a**, as the major configuration. n.d. = not determined.

Table 2:

Optimization of benzomorpholine formation.[a]

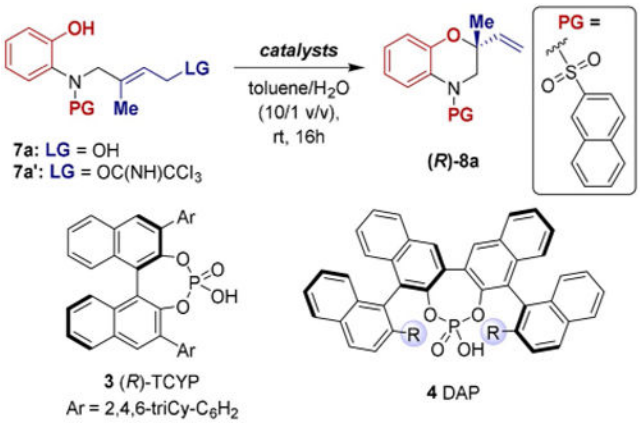

Entry	Substrate	Catalyst(s)	Conv. [%][b]	*ee* [%][c]
1[d]	**7a**	$Pd(PPh_3)_4$/**4a**	25	5
2	**7a**	$Pd(PPh_3)_4$/**4a**	72	9
3	**7a**	$Pd(PPh_3)_4$/**4c**	100	50
4	**7a**	$Pd(PPh_3)_4$/**4e**	59	86
5[e]	**7a**	$Pd(PPh_3)_4$/**4e**	100 (89)	93
6	**7a**	$Pd(PPh_3)_4$/**3**	trace	n.d.
7[d]	**7a′**	**4e**	24	−15

[a]The reaction was carried out with 10 mol% of $Pd(PPh_3)_4$ and/or CPA **3**/**4** in toluene/H_2O (10/1 v/v) at ambient temperature.

[b]Conv. represents conversion measured by crude ^1H NMR analysis, yields of isolated product in parentheses.

[c]*ee* of product **8a**, determined using HPLC equipped with a chiral column, wherein a positive ee corresponds to (*R*)-**8a**, and a negative *ee* to (*S*)-**8a**, as the major configuration. *n.d.* = not determined.

[d]Toluene was used as solvent.

[e]$PhCF_3/H_2O$ (10/1 v/v) was used as solvent, reaction duration 48 h.